Design and Testing of Planar Inverted-F Antennas with Application to the ORCASat CubeSat

Diogo Ribeiro Janeiro
diogo.janeiro@tecnico.ulisboa.pt

Instituto Superior Técnico, Universidade de Lisboa, Portugal

December 2021

Abstract

This thesis presents the development of an antenna to transmit telemetry from ORCASat, a two-unit CubeSat. The research includes four alternatives, followed by the in-depth analysis, manufacturing, and testing in an anechoic chamber of the selected configuration. The chosen design operates at 2.4 GHz and combines two Planar Inverted-F Antennas (PIFA) in a crossed configuration with a feeding port in the center and two shorting pins to tune the central frequency. This novel antenna design offers a linear polarization omnidirectional radiation pattern identical to a dipole antenna, but in a flat form factor, and without the need for a deployment system. Thus, the antenna eliminates deployment-associated risks and complexities. When mounted on the satellite end face, the antenna radiation pattern allows communication with Earth for every orientation of the satellite, making this design advantageous when dealing with the initial tumbling phase. Simulations of the antenna show a maximum gain of 2.8 dBi, a reflection coefficient of -29 dB at the 2.46 GHz working frequency and a 10 dB bandwidth of 54 MHz. The prototype was tested with a Virtual Network Analyzer (VNA) and the measured central frequency was 2.37 GHz, an error of 3.6%. The results in the anechoic chamber prove that the radiation pattern is omnidirectional.
Keywords: CubeSat, antenna, PIFA, radiation pattern.

1. Introduction

The space and telecommunication industries are booming and CubeSat projects such as ORCASat present an opportunity for university students to be part of these scientific and engineering developments.

ORCASat stands for Optical Reference Calibration Satellite. The payload of the two-unit (2U) CubeSat uses a laser to calibrate observation systems, eliminating measuring errors related with atmospheric interference. On-board of the satellite the intensity of the emitted light beam is registered, which is then compared with the value measured in the observatory in order to determine the effects of the atmospheric interference.

This project has the Canadian Space Agency (CSA) as the main stakeholder and it is led by the University of Victoria (UVic) Centre for Aerospace Research (CfAR).

This master thesis focuses on the development of alternate antenna designs for the ORCASat that do not require a deployment system, eliminating deployment associated risks and complexities, and prove to be tumbling resistant, meaning that the connection with the ground station is secured regardless of the orientation of the CubeSat.

The selected antenna alternative is designed for the next iteration of ORCASat, since the current CubeSat is in the final stages of development and is due to launch in 2022.

2. Background and Requirements

A brief recap of antenna theory is presented, followed by the antenna requirements for the ORCASat project and three examples of commonly used antennas for CubeSat applications.

2.1. Antenna Theory

According to the IEEE Standard Definitions of Terms for Antennas (IEEE Std 145–2013), an antenna is the component of a transmitting or receiving system that radiates or receives electromagnetic waves [12].

The Return Loss (RL) is the ratio of the power reflected at the antenna's terminals with the power that is fed from the transmission line [6], which can be expressed by

$$RL(dB) = -20log|\Gamma|, \tag{1}$$

where Γ is the reflection coefficient, given by

$$\Gamma = \frac{Z_i - Z_0}{Z_i + Z_0}, \tag{2}$$

where Z_0 is the characteristic impedance of the transmission line and Z_i is the input impedance of the matching circuit. When there is only one port, the return loss can be defined as the S_{11} parameter.

The impedance bandwidth at -10 dB (BW) is the difference between the upper and lower frequencies for which each intermediate value has a return loss lower than -10 dB.

Radiation patterns can be classified as isotropic, when radiation is uniform in all directions, directional when a specific direction is favored compared to others, and omnidirectional, a special type of directional pattern which is essentially non-directional in a given plane but has a directional pattern in any orthogonal plane [12].

The antenna directivity (D) is the ratio between the radiation intensity (U) per unit of solid angle and the mean value of the radiation intensity per unit of solid angle, which is equivalent to the ratio of the radiation intensity with the radiation intensity of an isotropic antenna with the same total radiated power (P_{ra}):

$$D(\theta, \varphi) = \frac{U(\theta, \varphi)}{< U(\theta, \varphi) >} = \frac{U(\theta, \varphi)}{P_{ra}/4\pi} \tag{3}$$

The antenna gain (G) is defined the same way as the directivity except instead of taking into account the radiated power, it is used the incident power (P_i) at the receiver, as shown in equation (4).

$$G(\theta, \varphi) = \frac{U(\theta, \varphi)}{P_i/4\pi} \tag{4}$$

The polarization can be characterized as linear or elliptical. Linear Polarization (LP) occurs when there is only one component Electric field (E) and elliptical polarization occurs when there is a combination of the two. Circular Polarization (CP) is a particular case of elliptical polarization where both components have the same magnitude, and it can be either Right-hand Circular Polarization (RHCP) or Left-hand Circular Polarization (LHCP).

2.2. Antenna Requirements

To summarize, the requirements for the new antenna are the following:

- Omnidirectional radiation pattern;
- G > 0 dBi;
- Same polarization type for the CubeSat's antenna and the ground station;
- Absence of moving parts;
- Area limited to 10×10 cm^2;
- Tumbling resistant;
- SNR > 13.8 dB;
- Working frequency in either the 435-438 MHz or the 2.40-2.50 GHz frequency bands;
- S_{11} < -15 dB;
- BW > 10 MHz.

2.3. Antenna Examples

In this section, three examples of commonly used antennas in CubeSat applications are introduced and characterized.

2.3.1 Monopole

A monopole is a one arm antenna that is typically the length of a quarter wavelength of the working frequency, $\lambda/4$. The size of the monopole antenna is around 3 cm at 2.45 GHz and 17 cm at 438 MHz, both cases rely on a deployment system, but in the case of the 2.45 GHz it is simpler to accomplish, given the smaller size.

The deployment system for monopole antennas usually involves the use of a nichrome wire that is heated to cut through a nylon wire, releasing the antenna, as described in [13, 14].

Monopole antennas can achieve above average return loss values, such is the case of the work presented in [9], where a 58cm antenna reaches -31.9 dB of return loss at a working frequency of 146 MHz and has a -15 dB impedance bandwidth of 9.5 MHz.

The monopole can also be used to take advantage of resonant frequencies, creating antennas with two distinct working frequencies, as the dual-band monopole shown in [11].

Monopoles use linear polarization, but circular polarization is possible resorting to a set of two monopole antennas perpendicular to each other.

The main limitations of this type of antennas are its dimensions and the use of deployment systems. Therefore, given the "absence of moving parts" requirement, monopole antennas are not further considered.

2.3.2 Patch

A patch antenna is composed of a metal plate, generally copper, on top of a substrate. This type of antennas is a flat form alternative to monopoles that does not rely on a deployment system.

In [10], a miniaturized UHF patch is manufactured and integrated in the BIRDS-1 CubeSat. This design uses a meander line, a shorting pin and a partial ground plane to lower and tune the working frequency to 437 MHz.

Circular polarization is achievable with methods such as the dual feed presented in [5], and the

cut corners of the metal plate of the patch presented in [8]. The antenna referred on [8] verifies that patches can comply with the frequency requirements, achieving a BW of 60 MHz and a return loss of -20 dB at 2.40 GHz.

This configuration of antennas is compact and offers reasonable values for the gain, BW and return loss, but lacks the broader radiation pattern that is required for the ORCASat's mission. This shortcoming may be compensated with the use of two patch antennas and therefore further research on this design is seen as beneficial.

2.3.3 PIFA

PIFA stands for Planar Inverted-F Antenna, a direct reference to the typical shape of this antenna. As described in [6], a PIFA can be obtained from a monopole by bending it 90°close to the ground plane. Then a shorting pin is added to enhance the impedance matching of the antenna. Instead of a wire, a wide metal plate can be used to increase the bandwidth. Figure 1 shows the referred design steps. If only a wire or a narrow metal plate is used, then it is considered an Inverted-F Antenna (IFA).

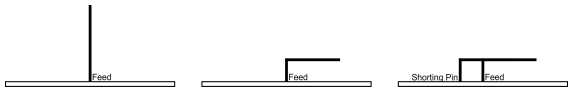

Figure 1: PIFA design[6].

The use of substrates between the PIFA and the ground plane can also reduce the size of the antenna, as it happens with the patch antennas.

The radiation pattern of the PIFA is not as ideal as the one offered by the monopole, but it is an improvement when compared to the patch, radiating more to the sides of antenna and to the back.

To obtain circular polarization it is necessary to use at least two PIFAs. In the work presented in [3], an array of four PIFAs generates circular polarization and achieves a 107 MHz BW with a -20.7 dB return loss at 2.35 GHz.

The work presented in [2] shows the four IFA array in the UHF band of the ANGELS 12U CubeSat. The array is tuned to 401 MHz with a return loss of -30 dB.

This type of antennas presents the required omnidirectional pattern as well as the other frequency, BW and return loss requirements. Moreover, it does not require moving parts and can be limited to one face of the CubeSat. Henceforth, the PIFA design is worth pursuing.

3. Design and simulation results

The designs of four different antennas were explored:

- S-band meshed patch antenna with CP that can be integrated with solar panels;
- S-band PIFA with CP;
- S-band crossed PIFA with an omnidirectional radiation pattern and LP;
- UHF crossed PIFA with an omnidirectional radiation pattern and LP.

3.1. S-band meshed antenna integrated with solar panels

An antenna that can be incorporated with a solar panel has the potential to be a valuable advantage, no longer being necessary to decide between antenna space and solar energy.

This approach is based on the work presented in [4]. The antenna was designed for the 2.40-2.50 GHz band and is circularly polarized, resorting to two orthogonal feed lines with a 90° phase difference.

The solar panel is simulated using a 98×82×1.1 mm^3 FR4 substrate ($\varepsilon_r = 4.4$), while a borosilicate glass substrate ($\varepsilon_r = 4.6$, $tan\ \delta = 37{\times}10^{-4}$) with a height of 3.5 mm is placed on top to hold the antenna. A transparent substrate such as the borosilicate glass is required in order for the light to reach the solar panel.

The meshed patch consists of seven horizontal and seven vertical lines with a width of 0.6 mm, length of 25.1 mm and a spacing of 3.48 mm. Two feed lines extend for 15 mm where a coaxial feed is placed through the substrates to the ground plane.

In order to compensate the high directivity of the meshed antenna, two antennas were placed on opposite sides of the CubeSat, as shown in Figure 2 (a).

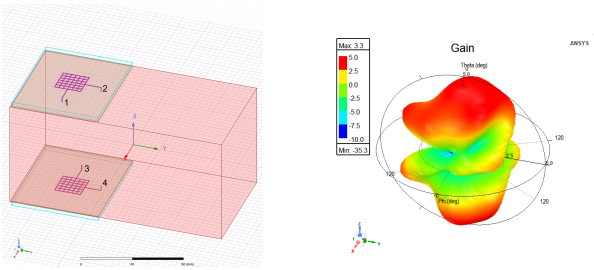

(a) Proposed design (b) Gain pattern

Figure 2: Two meshed antennas array.

The two meshed antennas maintain a working frequency of 2.46 GHz with a respective simulated S_{11} of -20.7 dB. The BW decreased 2 MHz to 62 MHz in total.

Despite the use of a second antenna, there are still considerable nulls around the radiation pattern in Figure 2 (b), which result from the interaction between the two antennas.

Regarding the CP, this was achieved with the two meshed antennas, having been measured maximum values of 2.1 dBi of RHCP and 0.4 dBi of LHCP.

The feed lines need to pass through the solar panels and reach the ground beneath them, which presents technical difficulties.

The case with the two antennas shows a radiation pattern with clear nulls along the sides of the CubeSat that do not have the antennas, making the configuration unsuitable.

3.2. S-band PIFA with circular polarization

Contrarily to patch antennas, PIFAs have omnidirectional radiation patterns, while still maintaining the reduced size necessary to fit the requirements.

In [1], a dual-band PIFA antenna is proposed. Given that the antenna's working frequencies are 868 MHz and 915 MHz, the necessary alterations were made to tune the antenna to the S-band.

The PIFA antenna consists of an 19.5×5×1.254 mm^3 elevated Rogers RO4003 substrate ($\varepsilon_r = 3.55$, $tan\ \delta = 27{\times}10^{-4}$) at a distance of 5.35 mm from the ground plane. The radiating patch on top of the substrate has a 16.6×1 mm^2 slot that stands 1 mm away from the feeding port. On the right side of the feeding port, there is another 0.5×1 mm^2 slot that connects to the main slot in the middle of the patch. A shorting pin was added on the left of the feeding port to tune the working frequency. The proposed design of the PIFA antenna can be seen in 3 (a).

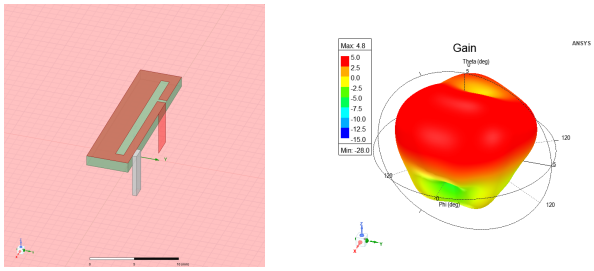

(a) Proposed design (b) Gain pattern

Figure 3: PIFA.

The PIFA antenna has a working frequency of 2.48 GHz with a respective simulated S_{11} of -18.9 dB and a BW of 30 MHz. The gain pattern in figure 3 (b) shows a maximum value of 4.8 dBi.

Two PIFAs were positioned on the corner of the top face of the Cubesat to test the viability of using the two antennas to emit CP, as shown in figure 4 (a). The PIFAs are placed as close to the edge as possible to free the space for an extra solar panel.

For this configuration the working frequency is 2.44 GHz with a corresponding simulated S_{11} of -24.1 dB and a measured BW of 87 MHz.

The two PIFAs were excited with a 90° phase difference to obtain CP. As shown in Figure 4 (b), a maximum gain of 6.2 dBi was obtained, mainly radiating in the -Y direction. In this case, both RHCP and LHCP maximum gain values are positive and above 1, 1.3 and 4.0 dBi respectively, therefore losses are to be expected when emitting CP.

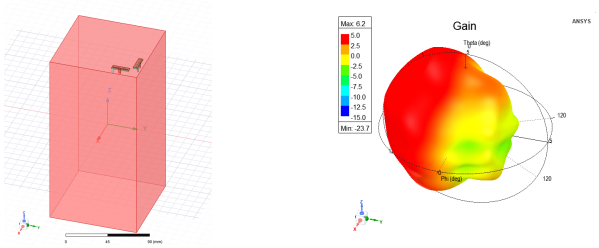

(a) Proposed configuration (b) Gain pattern

Figure 4: Different tested configurations for PIFA.

The case where the antenna is placed in the center of the face offers a reasonable omnidirectional radiation pattern, but slightly uneven.

Contrarily, the configuration with two PIFAs does not have an omnidirectional radiation pattern and therefore does not meet the requirements.

3.3. S-band crossed PIFA with linear polarization

A linearly polarized PIFA is explored in order to simplify the design and accomplish a more robust solution that is easy to manufacture.

Figure 5 (a) shows the proposed design for a novel crossed PIFA that consists of a crossed shape copper plate with a width of 5 mm and a side length of 30 mm on top of a 3.175 mm Rogers RT/duroid 5880 substrate ($\varepsilon_r = 2.2$, $tan\ \delta = 9{\times}10^{-4}$). The feeding port is placed in the center of the cross and two shorting pins are added 2 mm away from the feed.

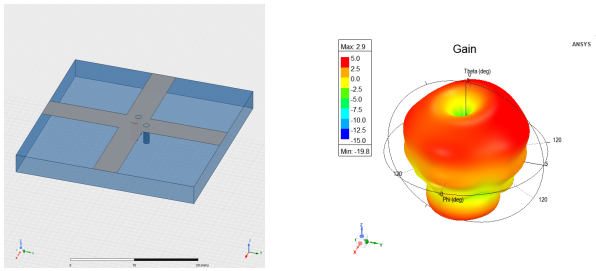

(a) Proposed design (b) Gain pattern.

Figure 5: Printed crossed PIFA with substrate.

The measured working frequency of the printed crossed PIFA is 2.46 GHz with a S_{11} of -17.4 dB and a 34 MHz BW. The maximum gain measured is 2.9 dBi and a omnidirectional radiation pattern was achieved, as seen in Figure 5 (b).

The crossed PIFA with the substrate and the printed copper plate has a height of only 3.175 mm, therefore obtaining a compact antenna with an

omnidirectional radiation pattern. Moreover, the PIFA can be easily produced by a PCB manufacturer, simplifying this process.

3.4. UHF crossed PIFA with linear polarization

Having a crossed PIFA with an omnidirectional radiation pattern in the 435-438 MHz band would be ideal, since the lower frequency would allow to use an antenna with a lower gain in the ground station to obtain the same P_r and SNR values as the 2.40-2.50 GHz band.

Miniaturization techniques are necessary to further lower the frequency of this antenna. The one implemented consists on rotating the PIFA 45° and creating a meander with each of the arms, as presented in figure 6 (a). Each arm has a width of 3 mm and is divided in ten 8 mm segments that are 4.5 mm apart and the offset of the shorting pins is 5 mm. Moreover, a high permittivity substrate is used with a 2 mm air gap between the antenna and the ground plane. The 2.5 mm Rogers RT/duroid 6010 substrate (ε_r = 10.2, $tan\ \delta$ = 23×10^{-4}) was selected, thus the height of the antenna amounts to 4.5 mm.

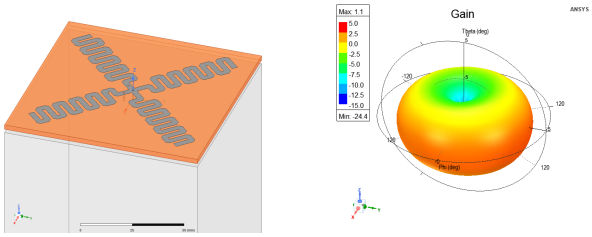

(a) Proposed design (b) Gain pattern

Figure 6: Meandered crossed PIFA with substrate.

The antenna has a working frequency of 436 MHz with a respective simulated S_{11} of -20.4 dB and a BW of 3 MHz. Figure 6 (b) shows the omnidirectional gain pattern of the antenna with a maximum value of 1.1 dBi.

The main disadvantage of the meandered crossed PIFA is the low impedance bandwidth that is below the 10 MHz requirement. However, the antenna itself can also be produced by a PCB manufacturer.

Moreover, the design can not produce CP.

3.5. Antenna selection

All the antennas were successfully tuned to either the 435-438 MHz or 2.40-2.50 GHz frequency bands, have a maximum gain higher than 1 dBi, and meet the S_{11} requirement of at most -15 dB. Furthermore, the antennas are restricted to a 10×10 cm^2 area and do not require any kind of deployment system or moving parts.

The two meshed patch antennas and the two-PIFA array offer CP, but at the same time these are the only antennas that do not have an omnidirectional radiation pattern and therefore can not be taken into further consideration.

The meandered crossed PIFA with substrate is selected to be further analyzed since it offers a omnidirectional radiation pattern and is easy to manufacture, even though it has an impedance bandwidth lower than what is required.

The printed crossed PIFA with substrate fulfills all of the referred requirements and is chosen for further analysis.

4. Detailed Antenna Characterization

This section presents the parametric analysis and coverage maps of the S-band and UHF PIFAs.

4.1. S-band Solution

There are four main parameters that affect the functioning of the 2.46 GHz printed crossed , these are the substrate thickness (h_1), the length of each of the four printed arms (dl), the width of the arms (W_{arm}) and the offset of the shorting pins in relation to the feed (offset). Thus, it is made a parametric analysis to measure the effects of alterations in these variables.

To determine whether the proposed antenna represents an improvement in regards to the typical patch antenna alternative, it is necessary to plot and compare the corresponding P_r and SNR coverage maps. For this purpose, a 42×42×3.175 mm^3 patch was simulated with the same Rogers RT/duroid 5880 substrate to use as reference. The resulting working frequency is 2.43 GHz with a respective simulated S_{11} of -31.4 dB and a BW of 62 MHz. The measured maximum gain is 8.2 dBi.

Before analyzing the coverage maps, a gain pattern comparison between the reference patch and the printed PIFA is made, as presented in figure 7. The plane used is perpendicular to the Earth's surface, corresponding to $\theta \in [-180°, 180°]$ and φ = 0°.

Out of the 360°theta sweep of the gain patterns in the plane perpendicular to the Earth's surface, the PIFA covers 191°and the patch 114°, which corresponds to 53 and 32% of the plane, respectively. Therefore, attending to this analysis, the PIFA is the superior alternative.

Figure 8 presents the gain pattern of the printed crossed PIFA in the plane that contains the antenna, which corresponds to $\theta \in [0°, 180°]$ and φ = 90°.

The gain oscillates between 0.6 dBi, for the directions perpendicular to the CubeSat's faces, and -0.8 dBi, for the directions of the edges. Therefore, the omnidirectional characteristic of this radiation pattern is evident in this plane.

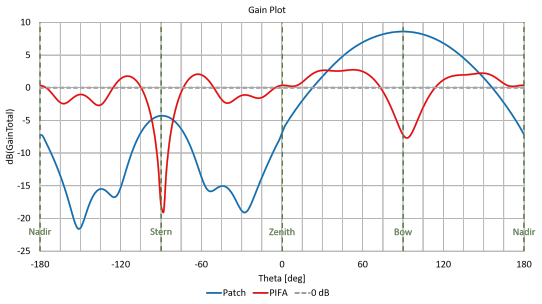

Figure 7: Gain patterns of the patch and the printed crossed PIFA for the plane perpendicular to the Earth's surface.

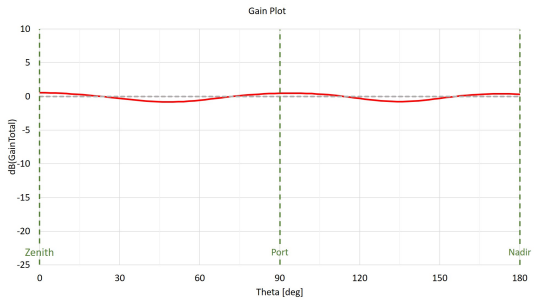

Figure 8: Gain pattern of the printed crossed PIFA for the plane that contains the antenna.

To simulate the coverage maps the following parameters were taken into consideration for both of the antennas:

- 5 W transmitted power;
- 400 km satellite orbit;
- 25 dBi ground station antenna gain;
- Map centered in Victoria, Canada, the location of the ground station, covering a total area of 1600×1000 km^2.

The ranges considered for the coverage maps are $P_r \in [-105, -85]$ dBm and SNR $\in [-10, 20]$ dB. Parts of the coverage maps that do not present colors signify a value below the minimum, if near a blue area, or above the maximum, if near a red area.

The directional characteristic of the reference patch antenna is evident on P_r coverage maps. In the Z direction the maximum gain of the patch is exposed, reaching -85 dBm of P_r in the center, the case where antenna is pointing to Nadir. Moreover, in the X direction the patch is pointing to Bow and therefore, the power that reaches the Earth's surface is significantly lower with a maximum of -89 dBm, and the minimum goes below -104 dBm.

On the other hand, the printed crossed PIFA shows a broader radiation pattern. In the X direction, for the P_r value of -96 dBm, the PIFA covers an area 1.5 times larger, as presented on table 1. In addition, in the Z direction the PIFA also covers a larger area for the same -96 dBm P_r value, about 1.3 times larger, even though the patch reaches a maximum P_r value that is 4 dBm higher.

The -Z direction reveals the most considerable difference between the two antennas. While the patch almost does not radiate backwards, showing a maximum P_r value of -97 dBm, the PIFA has a maximum P_r value of -89 dBm.

Table 1: P_r measured coverage area (S-band solution).

Antenna and Direction	Area above -96 dBm
Patch X	594×10^3 km^2
PIFA X	879×10^3 km^2
Patch Z	$1\ 174\times10^3$ km^2
PIFA Z	$1\ 501\times10^3$ km^2
Patch -Z	———
PIFA -Z	365×10^3 km^2

Both of the antennas reach the 13.8 dB mark for every direction.

Table 2 shows that for the -Z direction the reference patch antenna has an area above 13.8 dB that is 1.4 times larger than the printed crossed , which apparently contradicts the P_r results presented in table 1, but that is not the case. The reference patch antenna covers a larger 13.8 dB area because the part of the radiation pattern that points to the Earth's surface has a considerably lower gain, and thus a lower antenna noise power. Therefore, between the two antennas, the patch requires a lower P_r value to achieve the same SNR result for the -Z direction.

Contrarily, the opposite happens for the Z direction, when the antennas are pointing to Nadir. Since the patch has a higher gain than the , it also has a higher antenna noise power, which results on a smaller area above 13.8 dB of SNR.

Table 2: SNR measured coverage area (S-band solution).

Antenna and Direction	Area above 13.8 dB
Patch X	485×10^3 km^2
PIFA X	318×10^3 km^2
Patch Z	345×10^3 km^2
PIFA Z	356×10^3 km^2
Patch -Z	358×10^3 km^2
PIFA -Z	253×10^3 km^2

4.2. **UHF Solution**

There are six main parameters that affect the functioning of the UHF meandered crossed , these are

the substrate thickness (h_1), the height of the air gap (h_{gap}), the first part of the length of each printed arm (dl_1), the length of the meandered sections dl_2), the distance between meandered sections (movDist) and the offset of the shorting pins in relation to the feed (offset). A parametric analysis of these six variables is performed.

The same parameters as section 4.1 were used to obtain the coverage maps of the PIFA meandered crossed , changing only the gain of the antenna in the ground station from 25 to 10 dBi.

For the X and -Z directions, the PIFA reaches the P_r value of -96 dBm that was used as reference for the S-band solution and in both cases it covers an area larger than 600×10^3 km^2, as presented on table 3.

On the other hand, for the Z direction, the antenna does not surpass the -99 dBm P_r value. The antenna has a slightly asymmetric radiation pattern with a bigger gain pointing to the back of the PIFA than to the front side, which explains the lower measured values when the antenna is pointing to Nadir.

Table 3: P_r measured coverage area (UHF solution).

Antenna and Direction	Area above -96 dBm
PIFA X	667×10^3 km^2
PIFA Z	——
PIFA -Z	658×10^3 km^2

The UHF PIFA only reaches the 13.8 dB mark in the X direction, covering an area over 100×10^3 km^2, as presented on table 4.

Table 4: SNR measured coverage area (UHF solution).

Antenna and Direction	Area above 13.8 dB
PIFA X	115×10^3 km^2
PIFA Z	——
PIFA -Z	——

The results obtained for both solutions can be enhanced if needed by either increasing the transmitted power of the CubeSat antenna, that is limited to a maximum of 10 W in the case of ORCASat, or using a higher gain antenna in the ground station. Although, it is important to notice that in the case of the PIFA it would not be necessary to use a ground station antenna with a gain higher than 15 dBi, while in the case of the S-band , the 25 to 30 dBi ground station antenna would require powerful motors to steer it in the direction of the satellite.

The S-band printed crossed PIFA has fulfilled all the design requirements and therefore is ready to move to the prototype development stage.

5. Experimental Results

This section presents the design adjustments necessary to manufacture the antenna prototype, the assembly process and the experimental tests and results.

5.1. Design adjustments

The PCB manufacturer did not have in stock the 3.175 mm Rogers RT/duroid 5880 substrate (ε_r = 2.2, $tan\ \delta = 9\times10^{-4}$) that was used in the simulations. Therefore, it was necessary to choose a substrate that was available, in this case, the 1.524 mm Rogers RO4003C (ε_r = 3.4, $tan\ \delta = 27\times10^{-4}$).

After the substrate alteration, a 2 mm air gap was introduced in the model to increase the frequency and the BW. Moreover, the length of each arm was changed to 15.5 mm to tune the working frequency. The resulting frequency was 2.46 GHz with a respective simulated S_{11} of -29.1 dB and a BW of 54 MHz. The main differences of the new substrate are the increase of the BW by 20 MHz and the decrease of 12 dB of the S_{11} value for the same frequency.

Figure 9 shows the side view of the final simulated prototype design after the alteration of the substrate and the addition of the of the 2 mm air gap. The height of the antenna amounts to 3.5 mm.

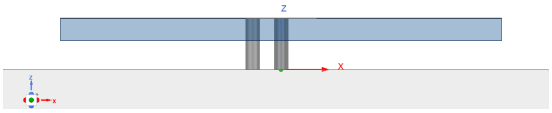

Figure 9: Side view of the printed crossed PIFA after the design adjustments.

The radiation pattern after the adjustments is consistent with the one prior, the only difference being a 0.1 dBi decrease of the maximum gain to a value of 3.0 dBi.

5.2. Prototype materials and assembly

The PCB that constitutes the PIFA antenna was designed in Altium Designer and the final file is presented on figure 10 (a), where one can observe the simplicity of the design. The green area corresponds to the Rogers RO4003C substrate and the brown to the copper plate. The circle in the center is the via where the feeding pin is placed and the other two circles are the vias for the shorting pins.

Figure 10 (b) shows the antenna manufactured by PCBWay [7].

The Amphenol RF MMCX connector model number 908-24100 was selected to link a coaxial cable to properly feed the antenna.

The presence of an air gap in this design demands for the addition of spacers to secure the antenna in place. Four 2 mm spacers made of acetal are used

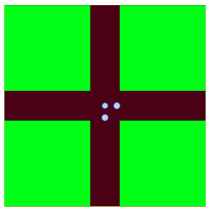

(a) PCB file

(b) Manufactured antenna

Figure 10: Printed crossed PIFA PCB.

in the corners of the PIFA and glued with epoxy.

The ground plane is made with a 0.4 mm copper plate that can be easily cut, drilled and soldered.

The assembling procedure of the PIFA is described.

Figure 11 shows two close up side views of the prototype after being assembled,where it can be observed that the three pins are not perfectly parallel to each other, which indicates that the holes of the ground plane are slightly misaligned with the holes of the PIFA.

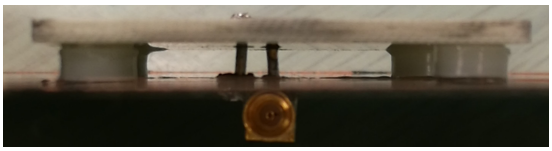

Figure 11: Side view of the connector and shorting pins.

5.3. **Frequency testing with VNA**

A Vector Network Analyzer (VNA) is used to measure the working frequency of the antenna and its impedance matching.

Figure 12 shows the S_{11} results from the VNA testing. The central frequency of the prototype is 2.37 GHz with a respective S_{11} of -44.6 dB and a BW of 68 MHz. The upper limit frequency of the impedance bandwidth is 2.40 GHz, which corresponds to the lower limit of the desired frequency band.

The frequency of the antenna is lower than the HFSS results by 88 MHz, corresponding to a 3.6 % error. This error is within what it expected for a first prototype of an antenna and does not imply an error in the design phase. Instead, it reveals the sensibility of the design to the assembly process. Therefore the final antenna must be rigorously assembled to assure the right working frequency and corresponding S_{11} values.

The -44.6 dB S_{11} value verifies that the impedance matching of the antenna was done correctly.

On the other hand, one can observe that the S_{11} line on figure 12 does not reach the 0 dB line on

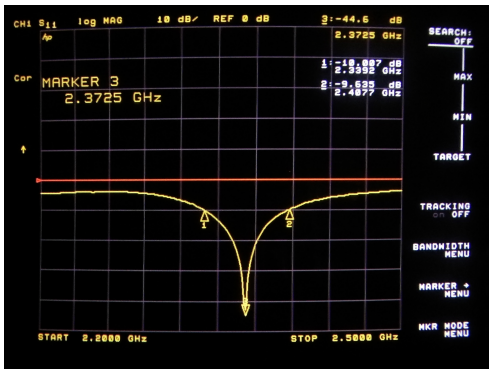

Figure 12: S_{11} results of the prototype PIFA.

the left and right parts of the graphic, revealing the existing of losses in the prototype. An error with the manufacturing is causing part of the antenna heat up unnecessarily, most probably related with the poor soldering and positioning of the MMCX connector and shorting pins.

The PIFA prototype was simulated in HFSS once again, but this time incorporating the design discrepancies between the assembled antenna and the previous simulation. The four acetal spacers were represented with a polyimide material ($\varepsilon_r = 3.5$, $tan\ \delta = 8{\times}10^{-3}$) and height of 2.4 mm, and only one face of the CubeSat was considered for the ground plane.

The simulated working frequency is 2.40 GHz with a respective S_{11} value of -21.5 dB and a BW of 54 MHz, showing that the unaccounted spacers in the simulation and the extra 0.4 mm in the air gap do indeed result on a decrease of the working frequency.

5.4. **Radiation pattern testing in an anechoic chamber**

A malfunction with the automatic positioner of the anechoic chamber of UVic hindered the testing of the radiation pattern of the prototype. Therefore, a second prototype was produced at IT, where it was possible to test the antenna in the anechoic chamber.

The second prototype was mounted on a copper plate square prism shape to simulate the 2U CubeSat structure. The copper body is connected to the antenna's prototype to extend the ground plane of the antenna to the surface of the structure.

Table 5 shows the frequency testing results with the VNA for the two prototypes.

Table 5: Frequency testing of the two prototypes.

Antenna	S_{11}	Frequency	Error
UVic's Prototype	-44.6 dB	2.37 GHz	3.6 %
IT's Prototype	-12.0 dB	2.45 GHz	0.4 %

The received power measurements for the PIFA were made in the anechoic chamber and a shift of 32 dB was applied to align and compare the simulation and experimental results. The shift corresponds to the estimated value of the scaling factor that converts the received power to the gain.

Figure 13 compares the simulated and experimental gain results of the PIFA for the plane perpendicular to the Earth's surface, corresponding to $\theta \in [-180°, 180°]$ and $\varphi = 0°$.

For $|\theta| > 130°$, the experimental values are lower than the simulation, which is due to the presence of the antenna positioner that blocks part of the measurements.

In the Bow direction, the null of the experimental results is more noticeable and wider. However, the remaining part of the radiation pattern is close to the simulated results.

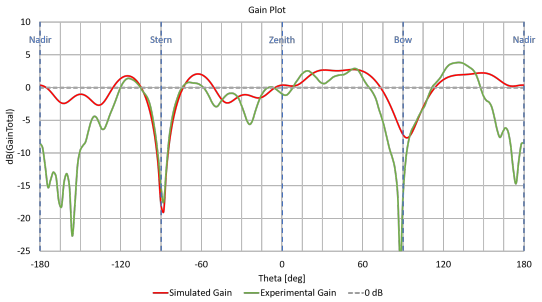

Figure 13: Simulated and experimental gain patterns of the crossed PIFA for the plane perpendicular to the Earth's surface.

Figure 14 compares the simulated and experimental gain results of the PIFA for the plane that contains the antenna, corresponding to $\theta \in [0°, 180°]$ and $\varphi = 90°$.

The experimental results show that the radiation pattern is omnidirectional as the simulation results indicated. In this plane, the positioner also obstructs part of the measurement of the received power for $\theta > 130°$.

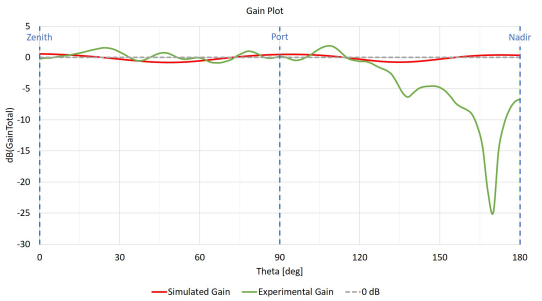

Figure 14: Simulated and experimental gain patterns of the crossed PIFA for the plane that contains the antenna.

6. Conclusions

This thesis focuses on the development of an antenna for CubeSat applications with an omnidirectional radiation pattern that is resistant to tumbling and does not rely on a deployment system or any moving parts. A list of requirements was compiled to evaluate the performance of the antenna in the scope of the ORCASat's mission. The selected antenna is designed to replace the current dipole antenna of the ORCASat in the next iteration of the project.

Four antenna configurations were simulated in HFSS obtaining different results and two designs were selected to be further analyzed, the S-band printed crossed PIFA and the UHF meandered crossed PIFA. Both these antennas present a novel design that combines two PIFAs in a cross pattern. The simulated measurements are a maximum gain of 2.9 dBi with a 2.46 GHz frequency and a corresponding S_{11} value of -17.4 dB for the S-band antenna, and a maximum gain of 1.1 dBi with a 437 MHz frequency and a corresponding S_{11} value of -20.4 dB for the UHF antenna.

A parametric analysis of the two PIFAs was performed where the impact of each design variable was examined. Furthermore, the coverage maps of both antennas were simulated to test if the SNR and radiation pattern requirements were met and to compare the results of the two solutions.

Even though the UHF PIFA requires a lower gain antenna in the ground station, when compared to the S-Band alternative, it also has a small impedance bandwidth at -10 dB of only 3 MHz. Thus, since the S-Band PIFA meets all the requirements and has an impedance bandwidth at -10 dB of 34 MHz, it was selected to be manufactured.

The material used for the antenna's PCB was changed since it was out of stock. Due to this alteration, a air gap was introduced in the design to tune the frequency with no negative impacts in the results. Afterwards, the prototype was assembled and frequency tested with a VNA, achieving an error of 3.6%, which is within the expected results for a first prototype.

A malfunction in the automatic positioner of the UVic's anechoic chamber prevented the measurement of the radiation pattern. As a solution, a second prototype was assembled at IT.

The anechoic chamber results show that the experimental radiation pattern's shape is close to the one simulated and therefore the antenna is omnidirectional.

6.1. Future Work

More work can be done to optimize the UHF meandered crossed PIFA design in order to increase the impedance bandwidth at -10 dB and consequently obtain a more robust antenna. If accomplished, the

same results of the S-band PIFA can be achieved without resorting to complex mechanisms of antenna steering in the ground station to track the CubeSat.

A suggestion to avoid errors in the assembly process of the antenna would be to manufacture a PCB for the ground plane with vias in the exact locations of the feeding and shorting pins.

The measurement of a reference antenna should be done in the anechoic chamber in the same conditions of the measurement of the second prototype in order to obtain the received power and calculate the gain of the crossed PIFA by comparison.

Further testing should be performed with the S-band printed crossed PIFA mounted on the CubeSat structure to evaluate the impact in the radiation pattern and working frequency of the antenna. If deemed necessary, additional tuning of the antenna can be performed to assure a working frequency within the 2.40-2.50 GHz band with a low corresponding S_{11}.

Acknowledgements
The author would like to thank Prof. Afzal Suleman and Prof. Carlos Fernandes for all the support given.

References

[1] K. Diallo, A. Ngom, A. Diallo, J. M. Ribero, I. Dioum, and S. Ouya. Efficient dual-band PIFA antenna for the Internet of Things (IoT). *2018 IEEE Conference on Antenna Measurements and Applications, CAMA 2018*, pages 0–3, 2018.

[2] R. Fragnier, L. Feat, R. Contreres, B. Palacin, K. Elis, A. Bellion, and G. L. Fur. Collocated Compact UHF and L-Band Antenna for Nanosatellite ARGOS Program. *13th European Conference on Antennas and Propagation, EuCAP 2019*, 2019.

[3] G. F. Kurnia, B. S. Nugroho, and A. D. Prasetyo. Planar inverted-f antenna (pifa) array with circular polarization for nano satellite application. In *2014 International Symposium on Antennas and Propagation Conference Proceedings*, pages 431–432. IEEE, 2014.

[4] Y. Li, S. K. Podilchak, and D. E. Anagnostou. A Miniaturized Circularly Polarized Antenna Using a Meandered Folded-Shorted Patch Array for CubeSats. *14th European Conference on Antennas and Propagation, EuCAP 2020*, 2020.

[5] X. Liu, J. Liu, D. R. Jackson, J. Chen, P. W. Fink, and G. Y. Lin. Broadband transparent circularly-polarized microstrip antennas for CubeSats. In *2016 IEEE Antennas and Propagation Society International Symposium, APSURSI 2016 - Proceedings*, pages 1545–1546. IEEE, 2016.

[6] A. Loutridis. *Study of UHF and VHF Compact Antennas*. PhD thesis, Technological University Dublin, 2015.

[7] PCBWay. Pcb prototype the easy way. https://www.pcbway.com/, 2021. (accessed: 24.10.2021).

[8] N. N. Rather and S. Suganthi. Electrically small S-band antenna for cubesat applications. In *Proceedings of the 2017 International Conference on Wireless Communications, Signal Processing and Networking, WiSPNET 2017*, volume 2018-Janua, pages 1687–1691, 2018.

[9] K. S. Sadasivan, S. N. Shalini, B. S. Cheela, and N. Annavarapu. Design and analysis of antennas for a nano-satellite. In *2017 IEEE Aerospace Conference*, pages 1–9. IEEE, mar 2017.

[10] M. Samsuzzaman, M. T. Islam, S. Kibria, and M. Cho. BIRDS-1 CubeSat Constellation Using Compact UHF Patch Antenna. *IEEE Access*, 6:54282–54294, 2018.

[11] K. Schraml, A. Narbudowicz, S. Chalermwisutkul, D. Heberling, and M. J. Ammann. Easy-to-deploy LC-loaded dipole and monopole antennas for cubesat. In *2017 11th European Conference on Antennas and Propagation, EUCAP 2017*, pages 2303–2306. IEEE, mar 2017.

[12] P. Society. Ieee standard definitions of terms for antennas. *IEEE Std 145-2013*, 2014.

[13] B. Takase. Novel Antenna Technologies for Small-Satellite and Terrestrial Applications. Master's thesis, University of Hawai'i, 2008.

[14] S. B. Zaki, M. H. Azami, T. Yamauchi, S. Kim, H. Masui, and M. Cho. Design, Analysis and Testing of Monopole Antenna Deployment Mechanism for BIRDS-2 CubeSat Applications. In *Journal of Physics: Conference Series*, volume 1152, page 012007, jan 2019.